

Surface modification of 316L Stainless steel by Sol-Gel method

A THESIS SUBMITTED IN PARTIAL FULFILLMENT
OF THE REQUIREMENT FOR THE DEGREE OF

**BACHELOR OF TECHNOLOGY
IN
BIO-MEDICAL ENGINEERING**

By

**ASISH KUMAR PADHI
(Roll No- 110BM0619)**



**DEPARTMENT OF BIOTECHNOLOGY & MEDICAL ENGINEERING
NATIONAL INSTITUTE OF TECHNOLOGY
ROURKELA
2013-2014**

Surface modification of 316L Stainless steel by Sol-Gel method

A THESIS SUBMITTED IN PARTIAL FULFILLMENT
OF THE REQUIREMENT FOR THE DEGREE OF

**BACHELOR OF TECHNOLOGY
IN
BIO-MEDICAL ENGINEERING**
By

**ASISH KUMAR PADHI
(Roll No- 110BM0619)**

Under the guidance of
Dr. Amit Biswas



**DEPARTMENT OF BIOTECHNOLOGY & MEDICAL ENGINEERING
NATIONAL INSTITUTE OF TECHNOLOGY
ROURKELA
2013-2014**

**NATIONAL INSTITUTE OF TECHNOLOGY
ROURKELA**

CERTIFICATE

This is to certify that the project titled “Surface modification of 316L stainless steel by sol-gel method” submitted by **Mr. Asish Kumar Padhi (110BM0619)** in the partial fulfillment of the requirements for the award of Bachelor of Technology in Bio-Medical Engineering during session 2010-2014 at National Institute of Technology, Rourkela and is an authentic work carried out by him under my supervision and guidance.

To the best of my knowledge the matter embodied in the thesis has not been submitted to any other University/Institute for award of any Degree/Diploma.

Date:
Place:

Dr. Amit Biswas
Assistant Professor
Department of Bio-Technology and Medical Engineering
National Institute of Technology
Rourkela-769008

Acknowledgement

I would like to take this opportunity to express my gratitude and sincere thanks to individuals who have been involved in my project & thesis work right from the initiation to the completion.

First of all I express my gratitude to my supervisor **Dr. Amit Biswas**, Assistant Professor of Department of Biotechnology and Medical Engineering, **NIT Rourkela**, for his esteemed guidance and noble supervision during the materialization of this work.

I would also like to thank all faculty members and staff of the Department of Biotechnology and Medical Engineering, N.I.T. Rourkela for their extreme help throughout the course of my project.

I would also like to thank my parents and my friends for their support and belief in me. I would especially like to thank Mr. **Chandra Prakash** and my friend **Sekharan Majhi** for all their help, without whom all this work would have been very difficult.

Asish Kumar Padhi
Roll no. –110bm0619
B.Tech(Bio-medical Engineering)

List of Abbreviations

SS : Stainless steel

Ti : Titanium

TiO₂ : Titanium dioxide

TBT : Tetra butyl-n-titanate

EAcAc : Ethyl acetoacetate

XRD : X-ray diffraction

OM : Optical microscopy

SBF : Simulated Body Fluid

LIST OF FIGURES

Fig 2.1 : Sol-gel method

Fig 3.1 : XRD system

Fig 3.2 : Optical microscope system

Fig 4.1 : Coated 316l ss samples

Fig 4.2 : TiO₂ diffraction peaks before sintering

Fig 4.3 : TiO₂ diffraction peaks after sintering

Fig 4.4 : Ground coated 316l ss sample

Fig 4.5 : Paper polished coated 316l ss sample

Fig 4.6 : Cloth polished coated 316l ss sample

Fig 4.7 : Cross sectional view of ground coated sample

Fig 4.8: Cross sectional view of paper polished coated sample

Fig 4.9 : Cross sectional view of cloth polished coated sample

Fig 4.10 : Apatite layer formed on ground coated sample

Fig 4.11 : Apatite layer formed on paper polished coated sample

Fig 4.12 : Apatite layer formed on cloth polished coated sample

Fig 4.13 : Apatite layer XRD peaks for ground coated sample

Fig 4.14 : Apatite layer XRD peaks for paper polished coated sample

Fig 4.15 : Apatite layer XRD peaks for cloth polished coated sample

LIST OF TABLES

Table 3.1 : Regents for preparing SBF (pH7.25, 1L)

Table 4.1 : Contact angle and surface energy of uncoated 316l ss samples

Table 4.2 : Contact angle and surface energy of coated 316l ss samples

LIST OF CONTENTS

Contents	page no
Abbreviations	v
List of figures	vi
List of table	vii
Abstract	x
 Chapter 1: introduction	 1
1.1 Introduction	2
 Chapter 2: Literature Review	 3
2.1 Biomaterials	4
2.2 surface modification and methods	5
2.3 sol-gel method	5
2.4 316l stainless steel	7
2.5 TiO ₂ coating	7
2.6 Objectives	8
 Chapter 3: Materials and methodology	 9
3.1 Methodology and work plan	10
3.2 preparation of 316l ss sample	11
3.2.1 cutting	11
3.2.2 grinding	11
3.2.3 paper polishing	11
3.2.4 cloth polishing	11
3.2.5 diamond polishing	11

3.3 preparation of TiO ₂ sol and coating material	12
3.4 characterization of the coated surface	13
3.4.1 XRD	13
3.4.2 Optical Microscope	15
3.4.3 Contact angle and surface energy	15
3.5 SBF bioactivity study	16
Chapter 4: Results and discussion	18
4.1 coating of the samples	19
4.2 contact angle and surface energy	20
4.3 X- ray diffraction	21
4.4 optical microscopy	23
4.5 SBF & bioactivity study	25
Conclusion	29
Reference	30

ABSTRACT:

Medical implants made from 316L stainless steel have been used widely and successfully for various types of dental and orthopaedic implants. It is believed that oxide films covering implant surfaces are of crucial importance for biocompatibility and successful osseointegration. A uniform TiO_2 coating on 316L stainless steel coupons has been prepared using sol-gel methodology followed by hydrothermal post-treatments. Sol-gel process is one of the best wet chemical routes to deposit the coating with convenient production of required thin films and controlled distribution of pore-size, processed at relatively lower temperature than any other conventional coating methods. Different coating thicknesses have been achieved by coating TiO_2 sol-gel on samples having different surface finish. The structure and morphology of the coatings were analyzed using optical microscope and X-ray diffraction technique. When the samples are observed under optical microscope, the results indicate that TiO_2 sol-gel coating on 316L stainless steel is uniform and dense; we can see a crack-free surface. The XRD patterns show different strong peaks of TiO_2 coating on the substrate. Bioactivity study of the coated samples is done by dipping them in SBF solution. We observe firmly attached hydroxyapatite layer on the TiO_2 coated substrate and XRD patterns show the presence of calcium phosphate which increases the osseointegration. The surface free energy has been calculated for the steel samples having different surface finish and also the contact angle has been measured. Ground samples show the best characteristics with enhanced roughness.

KEYWORDS- (TiO_2 , Sol-Gel, Hydroxy Apatite layer, Optical Microscopy, XRD, Surface energy, Coating angle)

CHAPTER 1

INTRODUCTION

1.1 INTRODUCTION:

316l stainless steel is the most common material implanted into the human body. This is widely applied as dental implants, bone fracture-fixation (pins, screws) and artificial joints (knee replacement, total hip replacement) due to their good mechanical properties, favorable biocompatibility and excellent corrosion resistance [1]. The surface properties of 316l ss implants influence biological responses at the interface between bone tissue and implants and, consequently, their osseointegration [2]; However, sometimes the interaction of these implants with the surrounding tissues cause complications including infection, inflammation, risk of rejection from implant-induced coagulation, allergic foreign body response, corrosion and wear. To overcome such complications, modification of surface of 316l ss is needed. Various types of coatings like zirconia, alumina, zirconia-alumina composite, TiO_2 coating are used these days on different substrates to be used in medical applications. TiO_2 coating is one of the suitable coatings capable of modifying 316l stainless steel surface. TiO_2 coatings are well suited as protective coatings in applications where additional benefits can be obtained through self-cleaning, anti-bacterial effects. This is applied extensively in the form of coatings, in particular for its unique properties such as non-toxicity, high photocatalytic activity, and super oxide forming capability on the surface. It enhances the anti-corrosion performance because of the formation of active oxide passivation layer and also restricts the formation of cracks on the surface of 316l ss which is to be used in fabricating the implants[3]. Sol-Gel process is one of the best wet chemical routes to deposit TiO_2 coating. This coating is chemically and photochemically stable and insoluble under normal pH conditions. Different coating methods can be used like plasma spraying, sputter deposition, dip coating and electrophoretic deposition to deposit TiO_2 coating. Here we are using the standard dip coating method to coat the 316l stainless steel surface. This TiO_2 coated 316l ss has many applications in medical field. These can be used as blood-contacting devices for improved blood compatibility [4]. They are one of the few biocompatible materials which osseointegrate, providing direct chemical or physical bonding with the adjacent bone surface without forming a fibrous tissue interface layer. For these reasons, they have been used successfully as orthopaedic and dental implants, for osteochondral, orthopedic, and osteo-progenitor implant applications[5].

CHAPTER 2

**LITERATURE
REVIEW**

2.1 BIOMATERIALS:

Biomaterials are any natural or synthetic materials, that have interaction with the living tissue and biological fluid and used to repair damaged parts of the body or to replace the damaged parts of the body. Its basic requirement is biocompatibility. Effective host response is produced by the biomaterials because of this biocompatibility for the application as per the requirement. Attractive and challenging research field of biomaterials have many applications to enhance the quality of life. Many complications arise when a biomaterial is implanted in the biological environment for the organ functions to be maintained or restored. For orthosis or prosthesis applications many medical devices are made from the biomaterials [6]. Different devices made from the biomaterials for medical applications include elbow, hip and dental implants, heart valve made artificially, eye lenses, artificial pancreas, artificial heart, and several types of bone implants. Metallic, polymeric, ceramic and composite biomaterials are used in medical applications. stainless steel is used for the heart valve, bone fixation, joint replacement and titanium and its alloys are used for dental bridge, joint replacement and dental implant formation. For dental filling, gold and silver is used for pacemaker wire, dental amalgams [7].

Different ceramic biomaterials used for the bio-medical application are:

Aluminum oxides for hip and dental implants, zirconia which is used for hip implants. calcium phosphate is used for bone graft substitutes and surface coating on the total joint replacements. Calcium sulfate, carbon are used for heart valve coating and orthopedic implant[8].

Different types of polymer biomaterials used for the biomedical applications are:

Nylon which is used for making surgical suture and tracheal tube, silicon rubber which is used for the formation of cell scaffold and fracture fixation, polyethylene which is used for formation of hip and knee joint and artificial tendons and ligaments[9].

2.2 SURFACE MODIFICATION AND METHODS:

Biomaterials implants which are fabricated for the purpose of commercial purchase, their surfaces are not so good with respect to their surface morphology, their phase purity and surface chemistry. Modifying the surface improves adhesion properties; micro-cleaning, functionality of amine, hydroxyl, carboxyl etc. After modifying the surface bio-compatible implants can be produced, which will have permanent wettability and also hydrophobic characteristics. These surface modification techniques, helps in shortening healing time and minimization of toxic reactions when the biological responses are directed in the proper cell or tissue function. Improvement of mechanical properties, reliability, stability and long-term performance of the medical device can be achieved by modifying the surface of biomaterials. Surface modification of biomaterials also provides ideal bulk properties to the surface of implant material (e.g. Tensile strength or stiffness) with the desired surface properties (e.g. Bio-compatibility or bio-activity)[10].

2.3 SOL-GEL METHOD:

The method involving the task of converting the monomers into a colloidal solution (sol) which will act as the precursor for integrated network (or gel) of either discrete particles or network polymers is known as Sol-Gel method. In this sol-gel process, the 'sol' (or solution) gradually evolves towards the formation of a gel-like diphasic system that contain both a liquid section and solid section. Its morphology ranges from discrete particles to continuous chemically active compound networks. Removal of the remaining liquid (solvent) requires a drying process, which results in a big quantity of shrinkage and concentration.

After the sol-gel is made, a heat treatment, or firing procedure, is often required for additional polycondensation and for enhancing mechanical properties and structural stability via final sintering. The precursor sol is either deposited on a substrate to form a film (e.g., by dip coating or spin coating), solid in to a desired form (e.g., to obtain monolithic ceramics, glasses, fibers, membranes, aerogels), or used to synthesize powders. This method of coating is a low-cost and low-temperature technique that permits for the fine control of the product's chemical

composition. It is used to manufacture uniform and thin films of metal oxides for various functions. Sol-gel derived materials have various applications in optics, physical science, energy, space, (bio)sensors, medicine (e.g., controlled drug release), reactive material and separation (e.g., chromatography) technology[11].

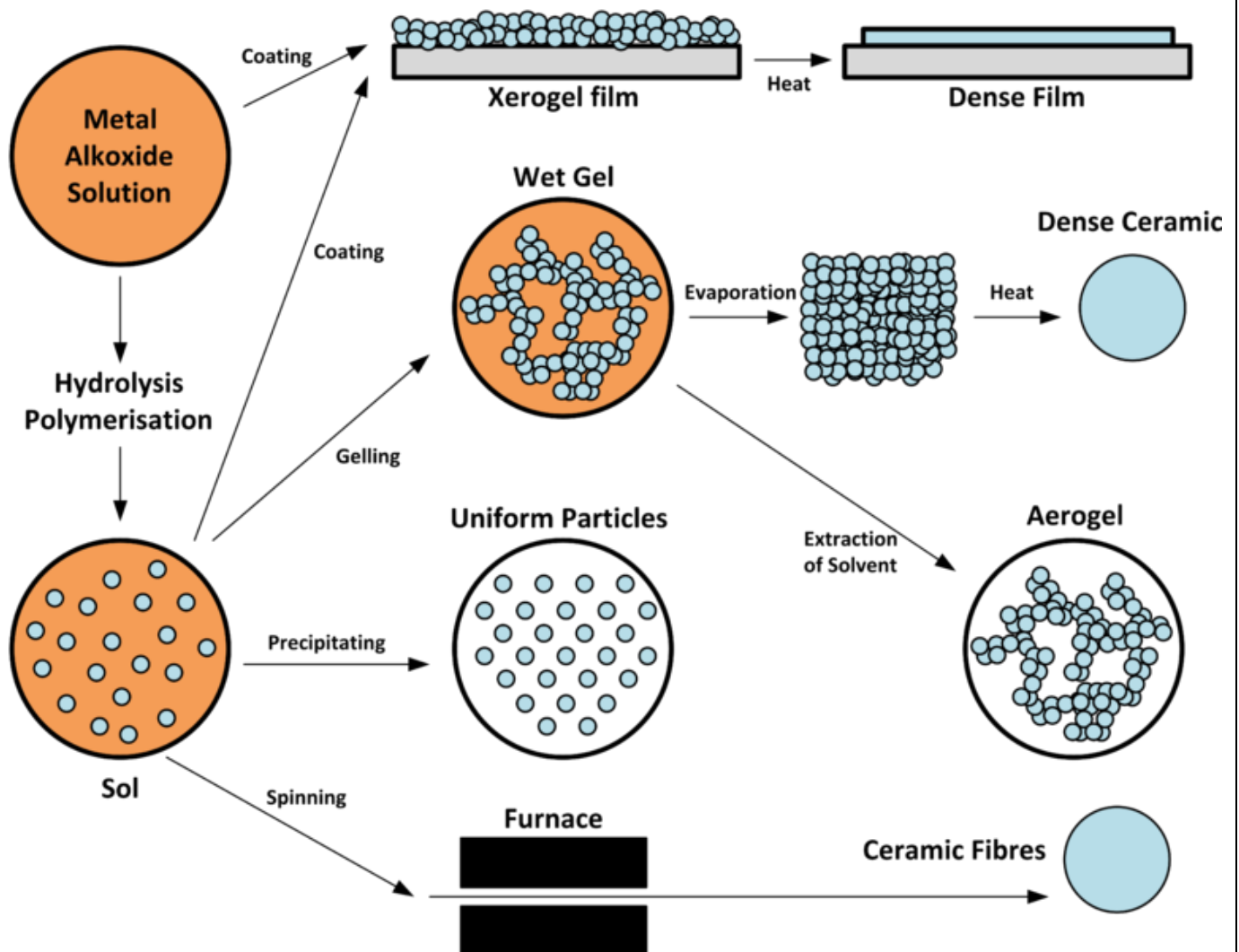


Fig 2.1- sol-gel method

2.4 316L stainless steel:

Stainless steel is additionally referred as “inox” steel. This type of steel does not show corrosion, wear or rusting or staining with water as normal steel does; however despite the name it is not absolutely stain-proof, most notably beneath low-oxygen, high-salinity, or poor-circulation environments. There are totally different grades and surface finishes of stainless steel to suit the setting the alloy should endure. 316L Stainless steel is employed wherever each of the properties of steel and resistance to corrosion are needed. Unprotected steels rust without delay when they are exposed to air and wet environment. This iron compound film (the rust) is active and it enhances corrosion by forming additional iron compound and with the increase of this compound, the film flakes and falls away. Stainless steels obstruct chemical element diffusion to the steel surface and blocks the corrosion of internal structure of the metal, which is because of the presence of enough Cr content [11].

2.5 TiO₂ Coating:

TiO₂ thin film coatings are either rutile TiO₂ or anatase TiO₂ or a mixture of both. These photocatalytic coatings show excellent anti-corrosion performance, they have strong self cleaning capability and anti bacterial effects. The deposition temperature varies from 50-600 degree celcius. Anatase TiO₂ shows a hardness of 2-5 GPa where as for rutile it is up to 15-20 GPa. Its thickness varies from 50 nm to 3 μm. It is stable under acid as well as alkaline conditions, especially when deposited at elevated temperature. Its photocatalytic activity depends on coating thickness and increases with the increase in coating thickness. It has strong anti-bacterial properties and 99% reduction of bacterial activity (E.coli) is observed for anatase coatings on steel. It has transparent color and depending on the coating thickness, interference colors appear [12].

2.6 OBJECTIVES:

- 1) To prepare TiO_2 sol-gel.**
- 2) To coat it on the steel coupons for producing crack free surface.**
- 3) To study bioactivity of coated samples using SBF solution.**

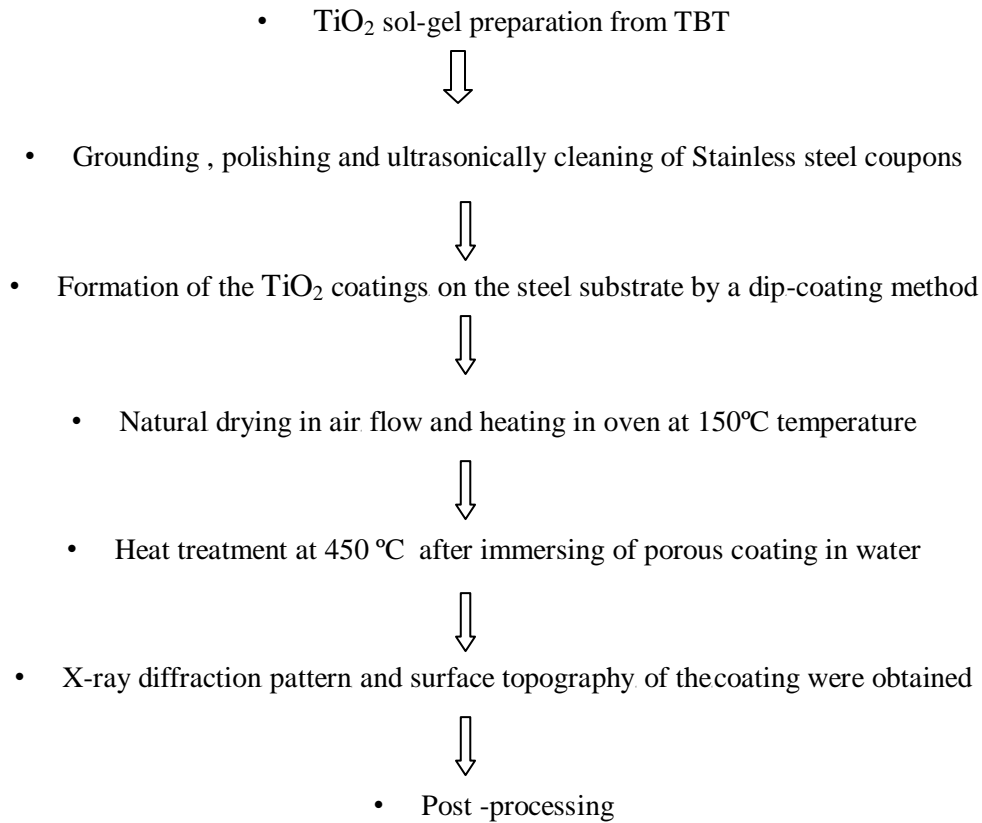
CHAPTER 3

MATERIALS

AND

METHODS

3.1 METHODOLOGY AND WORKPLAN



3.2 PREPARATION OF 316L SS SAMPLE:

3.2.1 Cutting

316l stainless steel samples were cut from an enough long stainless steel sheet in the dimension of 5mm×10mm×2.5mm. For cutting purpose of the samples hexa blades were used.

3.2.2 Grinding

Belt grinder was used for the grinding of the surface of the samples. Smoothly defined edges are made by this grinding process.

3.2.3 Paper polishing

Three types of emery papers named 1/0, 2/0 and 3/0 are used for the paper polishing purpose. Abrasive particles are there on the surface of these papers. 1/0 has highest roughness among the three types of papers. The roughness of the paper decreases from 1/0 to 3/0. Effective polishing was achieved by using two consecutive emery papers in the perpendicular fashion on the 316l SS samples. The particle roughness of the cut 316l SS samples is removed by the paper polishing method.

3.2.4 Cloth polishing

After polishing the samples with the emery papers, we perform cloth polishing. It was performed on a nylon pad which was attached on a cloth polishing wheel. Alumina paste was used as a polishing material in the cloth polishing. The scratches which remained after the samples were polished by emery papers are removed by cloth polishing process.

3.2.5 Diamond polishing

The final process of preparation of samples is diamond polishing. It is performed after we are done with polishing the samples in the cloth polish manner. It was performed only to remove the light lines and scratches which remained after cloth polishing. Diamond paste along with Hi-Fin spray was used in this process. A clean mirror-like surface is found on the surfaces of the samples after we perform diamond polishing.

3.3 preparation of TiO₂ sol and coating material:

TiO₂ sol was prepared from tetra-n-butyl titanate (TBT) according to the following process:-

1 ml ethanol and 1 ml ethyl acetoacetate (EAcAc) were mixed at room temperature. Then 4ml TBT was added to the solution and it was stirred continuously for 1 h. Within 30 min of the stirring, 0.2 ml of distilled water was added carefully to the solution for hydrolysis and then it was kept stirring for 10 h. The prepared yellow transparent solution was aged for 24 h before conducting coating on metal surface.

The 316L stainless-steel coupons were ground on the belt grinder for smooth edges, and polished with 1/0, 2/0 and 3/0 emery papers, then with Al₂O₃ powder, and at last cleaned ultrasonically in acetone and distilled water for 10 min, respectively. The TiO₂ coatings were deposited on the steel substrate by a dip-coating methodology at a withdrawal speed of 1 mm/s. Afterwards natural drying of the dip-coated samples was dried in air flow, and then the samples were heated at 150°C for 30 min. Such an operation was done to organize completely different coating thickness. Then, the specimens were treated thermally in an oven at 450°C for 30 min to change the chemical compound conversion and to get rid of the solvent and residual organics that remained on the coating, this was the final sintering. Elimination of crack defects within the coating and to optimize the coating structure, the samples with porous coatings were immersed in water for ten minutes, then dried in air flow again followed by final heat-treatment at 450°C for 10 min[13].

3.4 Characterization of the coated surface of the 316l ss sample:

3.4.1 X-Ray Diffraction (XRD)

Detailed information about the chemical composition and crystallographic structure of manufactured and natural materials is extracted by X-Ray diffraction (XRD) technique which is quite free from destruction. It can be used anywhere and it is user friendly. For characterizing and identifying the polycrystalline phases of different materials, we use powder diffraction method. Constructive interference is the basic principle of this X-Ray diffraction technique. Constructive interference can be explained as: when a monochromatic X-ray beam with wavelength λ is projected onto a crystalline material at an angle θ , diffraction occurs only when the distance travelled by the rays reflected from consecutive planes differs by a number n of wavelengths. When x-rays are scattered from a crystal lattice, peaks of scattered intensity are observed and which correspond to the following two conditions:

1. Incident angle = scattering angle.
2. The difference in path-length is equal to an integral multiple of wavelength.

In this XRD analysis graph is plotted between 2θ and counts [1-7]. In XRD analysis the Bragg's equation is considered.

$$n\lambda = 2d\sin\theta$$

where,

n is the number of wavelength,

λ is the wavelength,

d is spacing between the planes in the atomic lattice,

θ is the angle between the incident ray and the scattering planes.

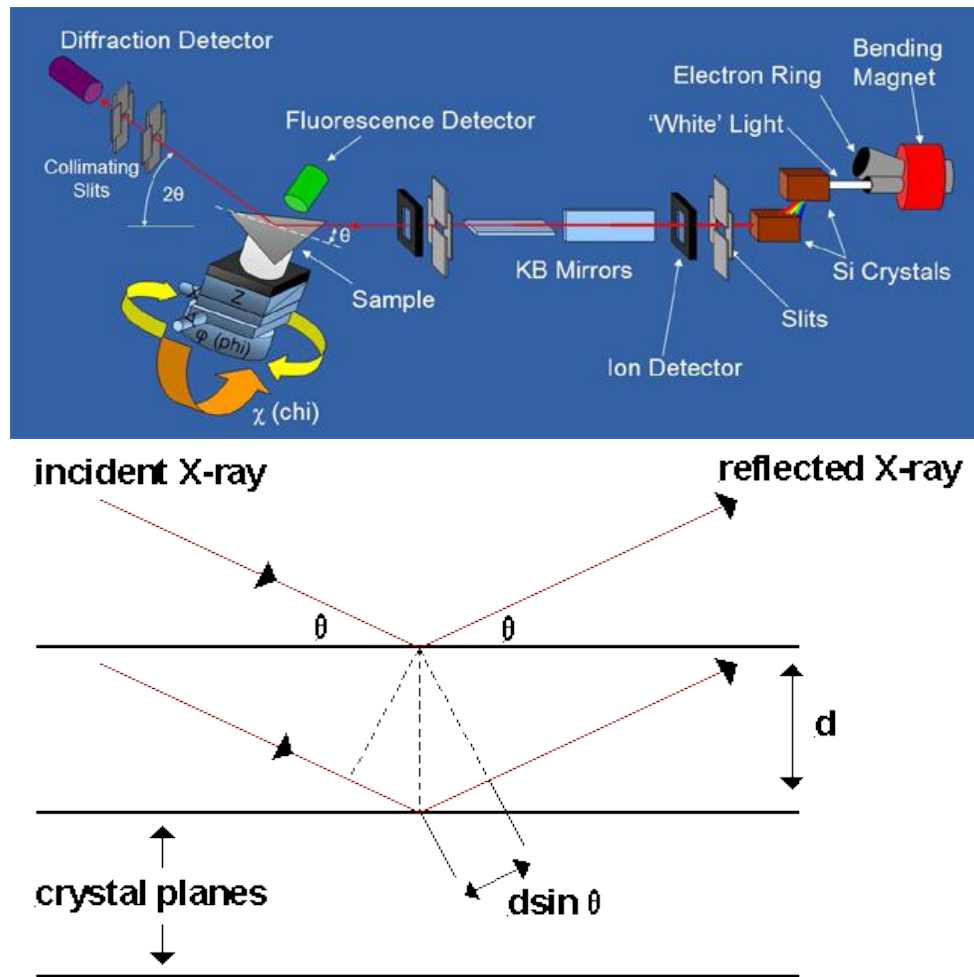


Fig 3.1 XRD system

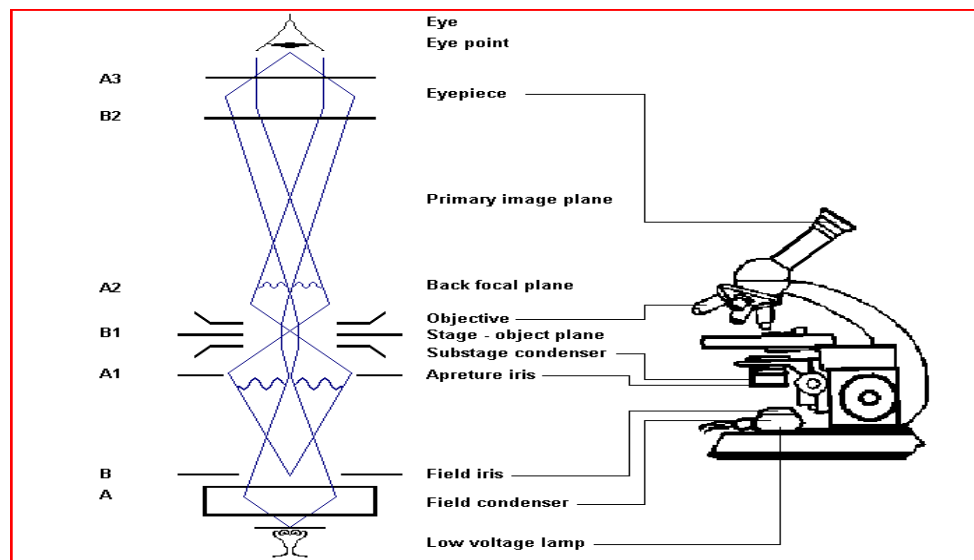


Fig 3.2 optical microscope system

3.4.2 Optical Microscope / Scanning Electron Microscopy (SEM)

The **optical microscope**, often referred to as the "**light microscope**". It can be of 2 types; simple and compound, is a type of microscope which uses visible light and a system of lenses to magnify images of small samples. It is used to check the surface morphology of the sample. Through this Optical microscope the surface topography of metal surface and deposited layer was analyzed by magnifying image. Whether crack is formed or not and the coating is uniform or not was also analyzed.

3.4.3 Contact angle and surface energy:

The **contact angle** is the angle, conventionally measured through the liquid, where a liquid/vapor interface meets a solid surface [14]. It quantifies the wettability of a solid surface by a liquid via the Young and Dupree equation. A given system of solid, liquid, and vapor at a given temperature and pressure has a unique equilibrium contact angle. However, in practice contact angle hysteresis is observed, ranging from the so-called advancing (maximal) contact angle to the receding (minimal) contact angle. The equilibrium contact is within those values, and can be calculated from them. The equilibrium contact angle reflects the relative strength of the liquid, solid, and vapor molecular interaction.

The theoretical description of contact arises from the consideration of a thermodynamic equilibrium between the three phases: the liquid phase (L), the solid phase (S), and the gas/vapor phase (G) (which could be a mixture of ambient atmosphere and an equilibrium concentration of the liquid vapor). The "gaseous" phase could also be another (immiscible) liquid phase. If the solid-vapor interfacial energy is denoted by γ_{SG} , the solid-liquid interfacial energy by γ_{SL} , and the liquid-vapor interfacial energy (i.e. the surface tension) by γ_{LG} , then the equilibrium contact angle θ_C is determined from these quantities by Young's Equation:

$$0 = \gamma_{SG} - \gamma_{SL} - \gamma_{LG} \cos \theta_C$$

The contact angle can also be related to the work of adhesion via the Young-Dupré equation: $\gamma(1 + \cos \theta_C) = \Delta W_{SLV}$. Where ΔW_{SLV} is the solid - liquid adhesion energy per unit area when in the medium V.

3.5 SBF BIOACTIVITY STUDY:

A **simulated body fluid** (SBF) is a solution with an ion concentration close to that of human blood plasma, kept under mild conditions of pH and identical physiological temperature. SBF was first introduced by Kokubo et al. In order to evaluate the changes on a surface of a bioactive glass ceramic[15]. Later, cell culture medium (such as DMEM, MEM, α -MEM, etc.), in combination with some methodologies adopted in cell culture, was suggested as an alternative to conventional SBF in assessing the bioactivity of materials. For an artificial material to bond to living bone, the formation of bonelike apatite layer on the surface of an implant is of significant importance. The SBF can be used as an *in vitro* testing method to study the formation of apatite layer on the surface of implants so as to predict their *in vivo* bone bioactivity. The consumption of calcium and phosphate ions, present in the SBF solution, results in the spontaneous growth of bone-like apatite nuclei on the surface of biomaterials *in vitro*. The SBF technique for surface modification of metallic implants is usually a time consuming process and obtaining uniform apatite layers on substrates takes at least 5 days with daily refreshing of the SBF solution.

Table 3.1 Regents for preparing SBF (pH7.25, 1L)

Order	Reagent	Amount
1	NaCl	7.996 g
2	NaHCO ₃	0.350 g
3	KCl	0.224 g
4	K ₂ HPO ₄ ·3H ₂ O	0.228 g
5	MgCl ₂ ·6H ₂ O	0.305 g
6	1M-HCl	40 mL
(About 90 % of total amount of HCl to be added)		
7	CaCl ₂	0.278 g
8	Na ₂ SO ₄	0.071 g
9	(CH ₂ OH) ₃ CNH ₂	6.057 g

A ground coated sample, a paper polished coated sample and a cloth polished coated sample are kept inside 3 different beakers containing 100 ml of SBF solution in each. It is left to form apatite layer on the coated surfaces for 5 days.

CHAPTER 4

RESULTS AND DISCUSSION

4.1 COATING OF THE SAMPLES :

After coating of the 316l ss samples, with TiO_2 sol gel, they are characterized for their surface morphology and phase purity. It can be seen that the coating is made thick and crack-free, it is uniform and dense.

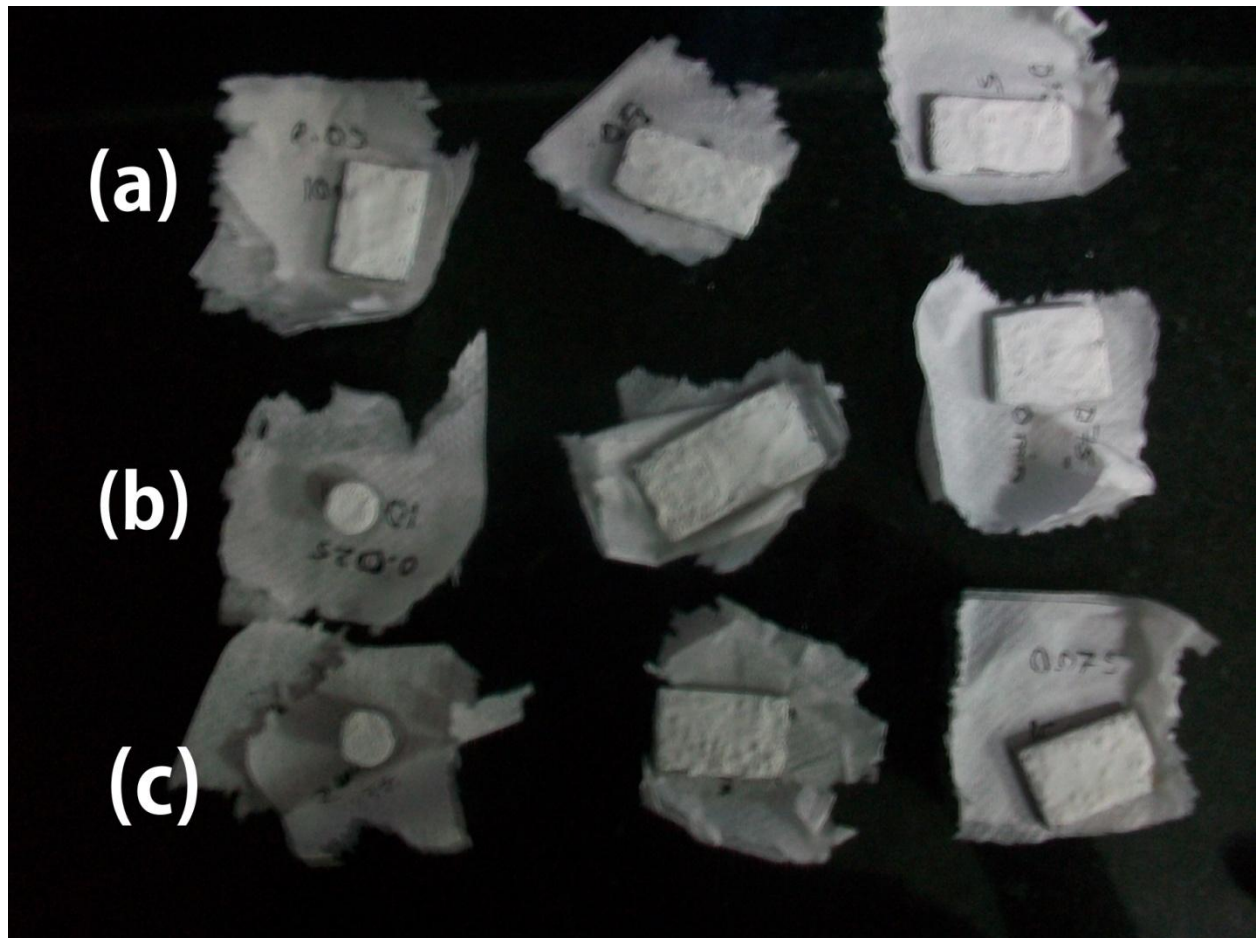


Fig 4.1: TiO_2 coated 316l SS substrated with 3 different level of surface finish.

(a) Ground, (b) Paper polished, (c) Cloth polished

4.2 CONTACT ANGLE AND SURFACE ENERGY:

Contact angle and surface energy of the samples were found using the KRUSS system and software taking water as the liquid. As we know roughness values of ground samples are more and cloth polished samples have less roughness values. So accordingly contact angle and surface energy of the samples before and after coating the samples were found.

Table 4.1: Contact angle and surface energy of uncoated 316l ss samples:

	Contact angle	Surface energy
Cloth polished samples	63.33	43.1 mN/m
Ground samples	45.53	32 mN/m

Table 4.2: Contact angle and surface energy of coated 316l ss samples:

	Contact angle	Surface energy
Cloth polished samples	85.51	55.8 mN/m
Ground samples	67.75	43.1 mN/m

From Table 4.1, we get contact angle and surface energy of cloth polished and ground uncoated 316l SS. It shows that as roughness decreases, it results in higher contact angle, From Table 4.2 we get contact angles and surface energy of cloth polished and ground TiO₂ coated 316l SS showing that less roughness results in higher contact angle and after the coating is done, surface energy increases.

4.3 X-RAY DIFFRACTION:

The diffraction patterns were obtained using ULTIMA IV instrument, for the Non-sintered and sintered coated samples.

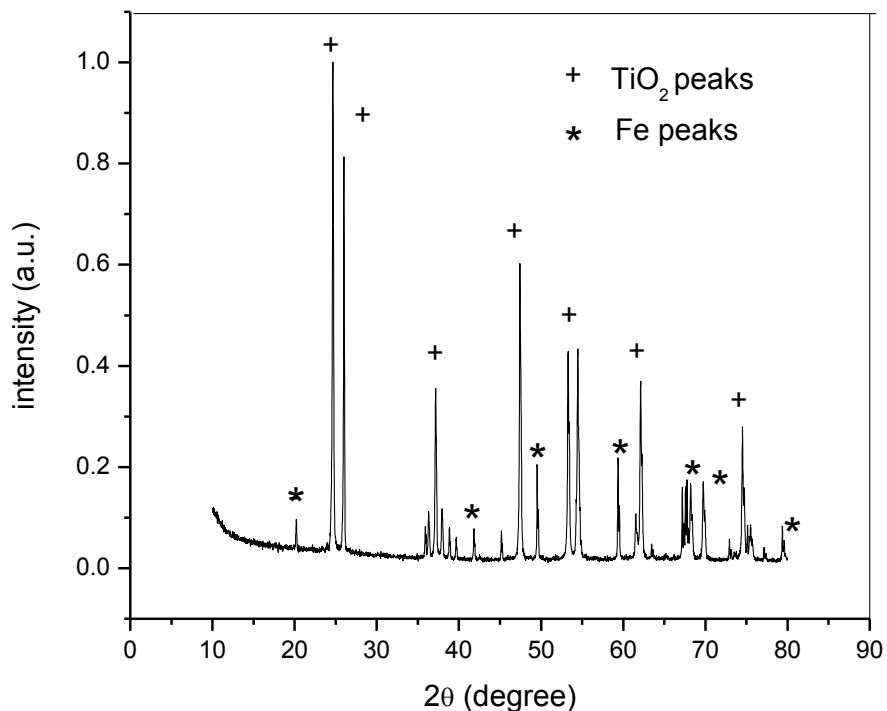


Figure 4.2: TiO₂ XRD diffraction peaks before sintering along with the Fe peaks

For the non sintered samples, the strong diffraction peaks were obtained at $2\theta = 24.66, 26, 37.18, 47.42$ (in degrees), along with Fe (Austenite or gamma iron) peaks. It follows the JCPDS data code 82-0514 of the rutile phase of TiO₂, showing TiO₂ is in crystallized form and Fe is in its most stable form i.e. gamma iron.

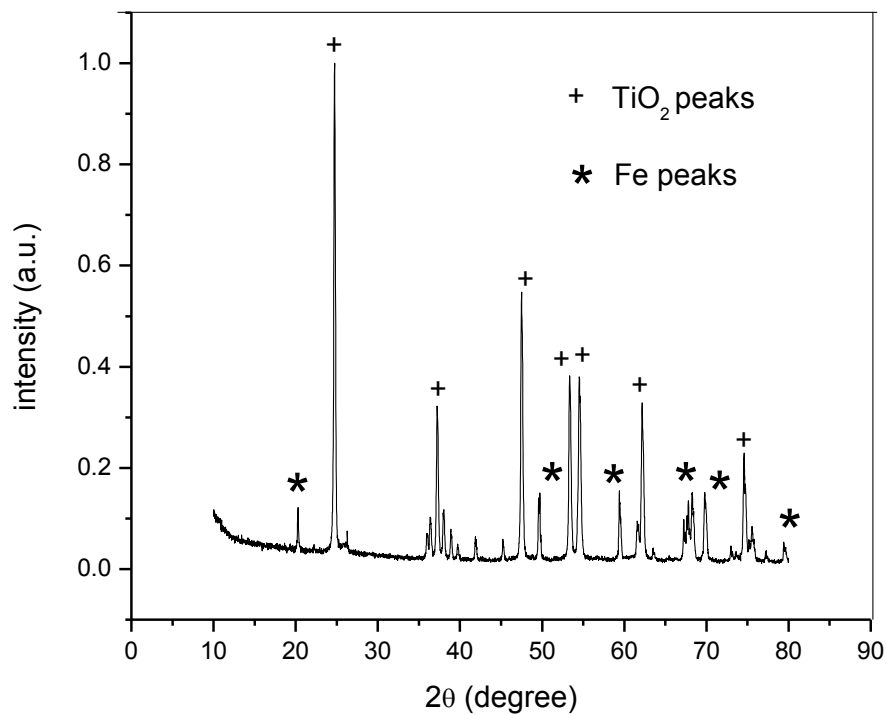


Figure 4.3: TiO₂ XRD diffraction peaks after sintering along with the Fe peaks

For the sintered samples the strong diffraction peaks were obtained at $2\theta=24.9, 36.7, 48, 53.6$ (in degrees), along with Fe (Austenite or gamma iron) peaks, it follows the JCPDS data code 84-1286 of the rutile phase, with strong peaks for TiO₂. It shows that after sintering the coated samples, the final compaction and crystallization of TiO₂ coating occurs.

4.4 OPTICAL MICROSCOPY:

The coated samples were observed under the optical microscope, their surface characterization was done, taking pictures of the surface at higher magnification and from their cross-sectional pictures, we could find the coating thickness, for different samples with different roughness values. It is concluded that, the coating is made crack free after observing the pictures.



Fig 4.4 : Coated surface of Ground 316L ss sample



Fig 4.5 : Coated surface of Paper polished 316L ss sample



Fig 4.6: Coated surface of cloth polished 316L ss sample

From the above figures(fig 4.4, fig4.5) the ground and paper polished samples have globular coating deposition with particle cluster size is about 40 nm., in Fig 4.6, we can observe particulate deposition on cloth polished 316L ss sample and coating is made uniform and dense, particle size about 35nm.

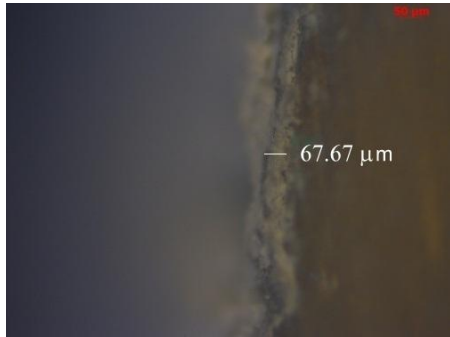


Fig 4.7 Cross sectional view of ground coated sample



Fig 4.8 Cross sectional view of paper polished coated sample

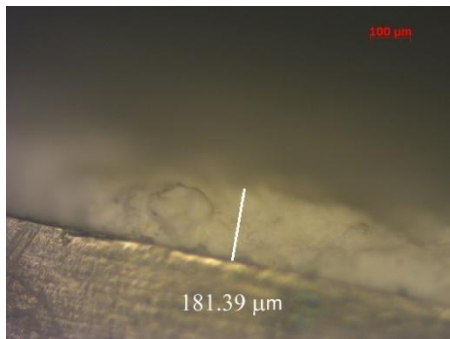


Fig 4.9 Cross sectional view of cloth polished coated sample

Thickness of TiO_2 coating of ground, paper polished and cloth polished samples are 67.67 μm (Fig 4.7), 122.4 μm (Fig 4.8), and 181.39 μm (Fig 4.9), respectively.

4.5 SBF BIOACTIVITY STUDY:

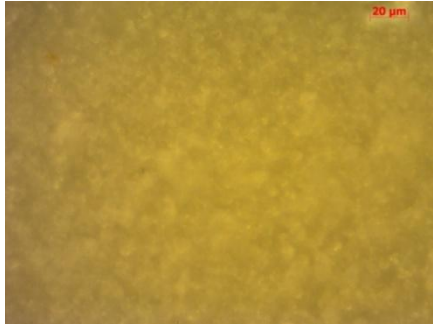


Fig 4.10: Apatite layer formed on ground coated sample

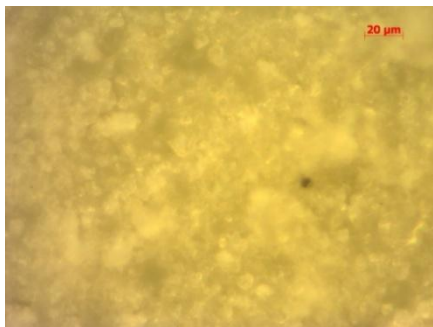


Fig 4.11: Apatite layer formed on paper polished coated sample

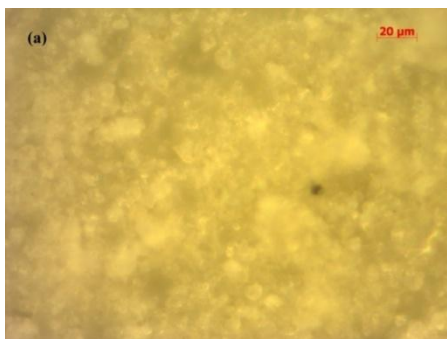


Fig 4.12 : Apatite layer formed on cloth polished coated sample

Fig 4.10, Fig 4.11, Fig 4.12 : A ground coated sample(Fig 4.10), a paper polished coated sample(Fig 4.11) and a cloth polished coated sample(Fig 4.12) are kept inside 3 different beakers containing 100 ml of SBF solution in each. It is left to form apatite layer on the coated surfaces

for 5 days, and at the end of 5th day when the layers are formed first we took the samples for optical microscopy test and found the pictures of the apatite layer, it is crack free and uniform, on the ground coated sample it is continuous deposition of apatite layer, but on the paper polished coated sample and cloth polished coated sample it is particulate coating deposited. Particle size is about 750 nm.

After the optical microscopy test, the samples were taken for X-Ray diffraction test, and strong peaks were found for the formed apatite layer on the coated samples. It was seen that,

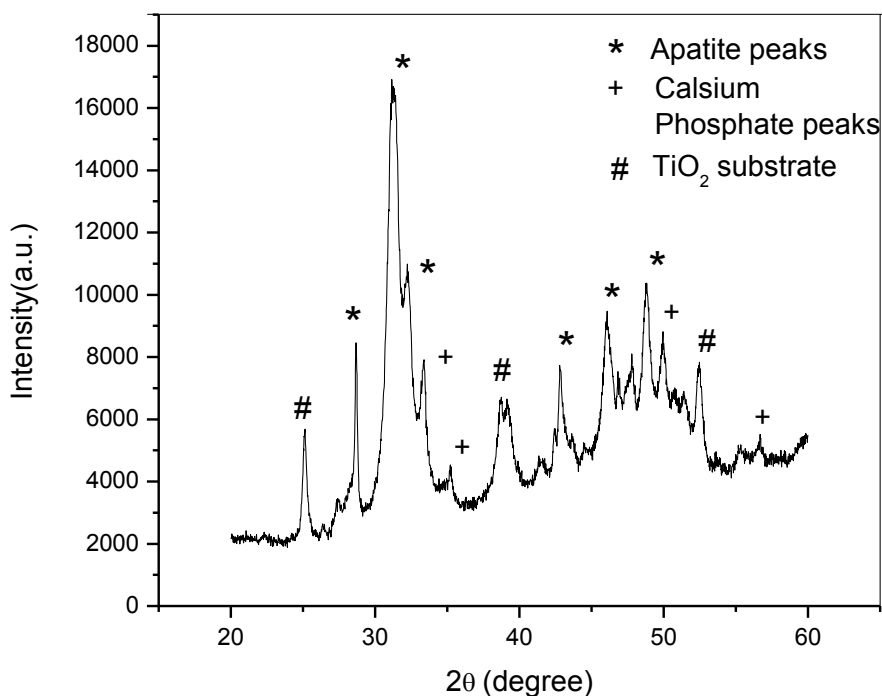


Fig 4.13: Apatite layer XRD peaks for ground coated sample

For ground coated samples the strong peaks were found at $2\theta = \{24.9, 31, 32.1\}$, it follows the JCPDS data code 21-839 that states the presence of calcium phosphate along with apatite, which results in better osseointegration of the coated sample when implanted inside human body.

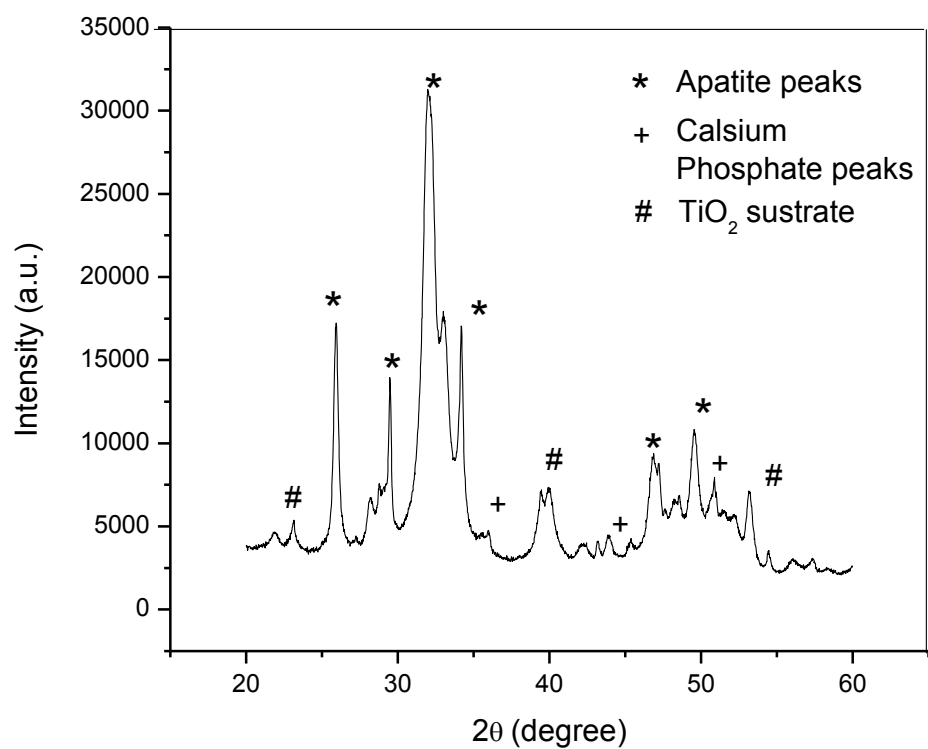


Fig 4.14: Apatite layer XRD peaks for paper polished coated sample

For the paper polished coated samples strong peaks were found at $2\theta = \{26, 32, 33\}$ (Fig 4.14) and it follows the JCPDS data code 21-839 showing presence of calcium phosphate.

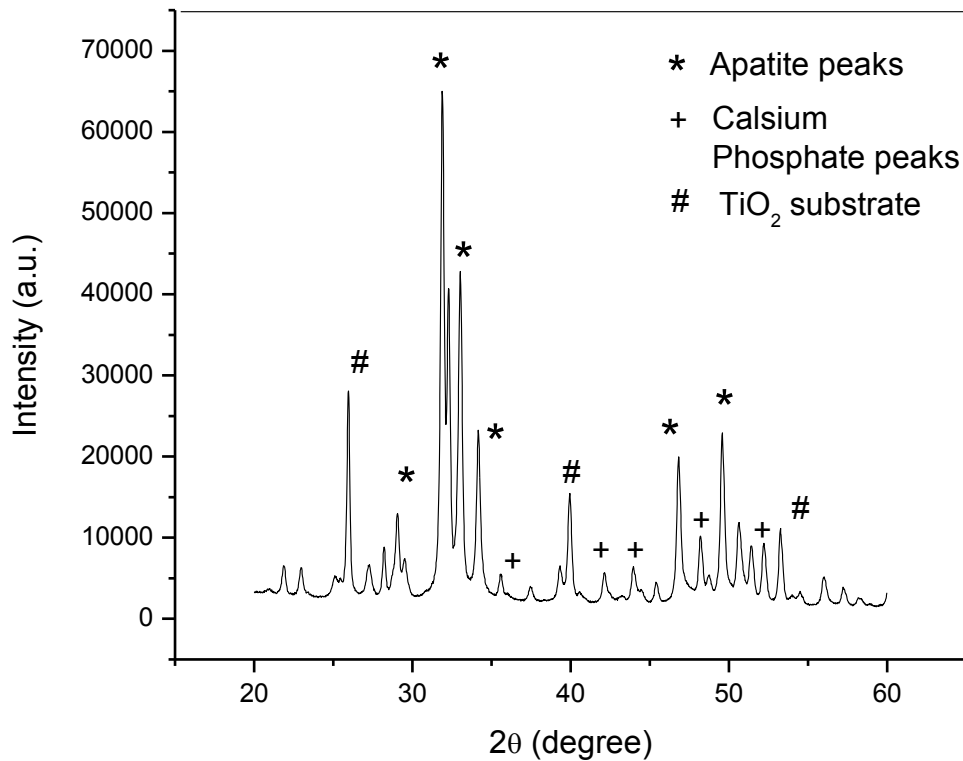


Fig 4.15: Apatite layer XRD peaks for cloth polished coated sample

For the cloth polished coated samples strong peaks were found at $2\theta = \{25.9, 31.8, 32.3\}$ (Fig 4.15) and it also follows the JCPDS data code 21-839 showing presence of calcium phosphate along with apatite which enhances the osseointegration of the implants while forming bonds with surrounding bones and tissues.

CONCLUSION

A Smooth and uniform TiO_2 coating on the 316 L stainless steel has been prepared by the sol-gel method followed by a hydrothermal post-treatment. It is observed from optical microscopy that the coating is made uniform, dense and crack free. The XRD test on the coated samples reveals the strong diffraction peaks of TiO_2 . Finally SBF and bioactivity study was performed for 5 days, and it shows the Hydroxyapatite layer formed on the coated surface which can increase the tendency to form bond with the bones when implanted inside the human body and the presence of calcium phosphate can enhance the osseo-integration.

REFERENCE

- [1] N. Eliaz¹, T. M. Sridhar, U. Kamachi Mudali , Baldev Raj, Surface Engineering VOL 21 NO 3 (2005), DOI 10.1179/174329405X50091.
- [2] M,wei, A.J.ruys, M.V.swain, S.H.kim, B.K.milthorpe, C.C.sorrel, Journal of materials science :materials in medicine 10 (1999) 401-409
- [3] A.A. Abdeltawab , M.A. Shoeib , S.G. Mohamed , J. Surface & Coatings Technology 206 (2011) 43–50.
- [4] C.T. Kwok , P.K. Wong, F.T. Cheng, H.C. Man, Applied Surface Science 255 (2009) 6736–6744.
- [5] M. Javidi, S. Javadpour , M.E. Bahrololoom , J. Ma , J. Materials Science and Engineering C 28 (2008) 1509-1515.
- [6] A. R. Boccaccinia , I. Zhitomirskyb, J. Solid State and Materials Science 6 (2002) 251-260.
- [7] K. Dong-Yoon, K. Miyoung, K. Hyoun-Ee, K. Young-Hag,K. Hae-Won,J. Jun-Hyeog, J.Acta Biomaterialia 5 (2009) 2196–2205.
- [8] L. Changjian ,H. Huijuan, Z.Fang, L Aimin, J Mater Sci: Mater Med (2008) 19:2569–2574 ,DOI 10.1007/s10856-007-3196-1.
- [9] A. R. Boccaccini, S. Keim, R.Ma, Y. Li, I. Zhitomirsky, J. R. Soc. Interface (2010) 7, S581–S613.
- [10] A.Onder, O. Cinar, T. Mustafa, A. Sabri, Rev.Adv.Mater.Sci. 15(2007) 10-15.
- [11] S. Radice, H. Dietsch, S. Mischler, J. Michler, Surface & Coatings Technology 204 (2010) 1749–1754.
- [12] O. Albayrak, S. Altintas, J. Mater. Sci. Technol., (2010), 26(11), 1006-1010.
- [13]X. Liu, Ray W.Y. , S. C.H. Kwoka, K. C. Paul, C. Ding, Surface & Coatings Technology 186 (2004) 227– 233
- [14]H.X. Wang, S.K. Guan, X. Wang, C.X. Ren, L.G. Wang, Acta Biomaterialia 6 (2010) 1743–1748
- [15] B. Viswanath, N. Ravishankar, Biomaterials 29 (2008): 4855–63.